SUPPORTING INFORMATION FOR

Conformational dynamics and self-association of intrinsically disordered Huntingtin exon 1 in cells

Steffen Büning[a*], Abhishek Sharma[a*], Shivang Vachharajani[a*], Estella Newcombe[b], Angelique Ormsby[b], Mimi Gao[a], David Gnutt[a], Tobias Vöpel[a], Danny M. Hatters[b], Simon Ebbinghaus[a]

Author affiliation: [a]Department of Physical Chemistry II, Ruhr-University Bochum, Universitaetsstraße 150, D-44780 Bochum, Germany. [b]Department of Biochemistry and Molecular Biology & Bio21 Molecular Science and Biotechnology institute, University of Melbourne, Melbourne, Australia.

Corresponding author: Correspondence should be addressed to Simon Ebbinghaus, ++49 234 3225533, Simon.Ebbinghaus@rub.de, * These authors contributed equally.

SUPPLEMENTARY FIGURES

Supplementary Figure S1

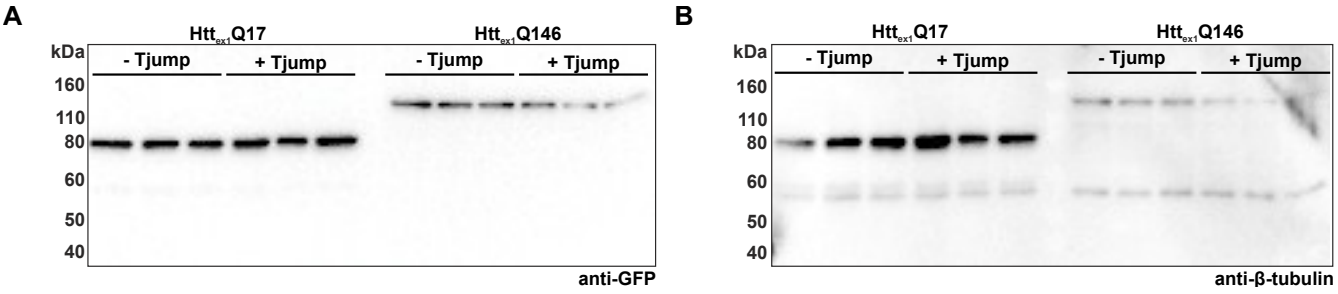

Western Blots of the lysates of HeLa cells transfected with $Htt_{ex1}Q17$ (67 kDa) and $Htt_{ex1}Q146$ (83 kDa).

Three pockets of the gel were loaded with lysate of each transfected construct after incubation at 45 °C for 6 min (+ Tjump) and without incubation at 45 °C (- Tjump). (*A*) Stained Blot after the incubation with the anti-GFP primary antibody. The difference between the visible bands and the calculated mass can be attributed to the retarding effect of the polyQ tract [1]. (*B*) Stained Blot after stripping the GFP panel and incubation with the control anti-β-tubulin primary antibody.

Supplementary Figure S2

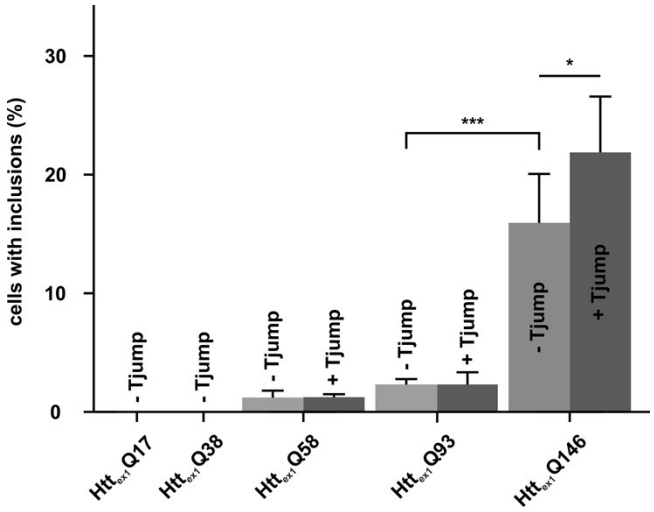

Inclusion body formation in AcGFP1-Htt$_{ex1}$-mCherry transfected cells

Relative abundance of cells containing inclusion bodies 16 - 20 hours after transfection. Total number of cells counted: Htt$_{ex1}$Q17 (n=262, two replicates), Htt$_{ex1}$Q38 (n=155, two replicates), Htt$_{ex1}$Q58 (n_{-Tjump}=1417, n_{+Tjump}=1560, four replicates each), Htt$_{ex1}$Q93 (n_{-Tjump}=1279, n_{+Tjump}=1201, four replicates each), and Htt$_{ex1}$Q146 (n_{-Tjump}=1473, n_{+Tjump}=1276, four replicates each). The error bars were calculated as SD and the statistical significance was tested by a one-way ANOVA with post-hoc Tukey test. * $p < 0.05$, ** $p < 0.01$

Supplementary Figure S3

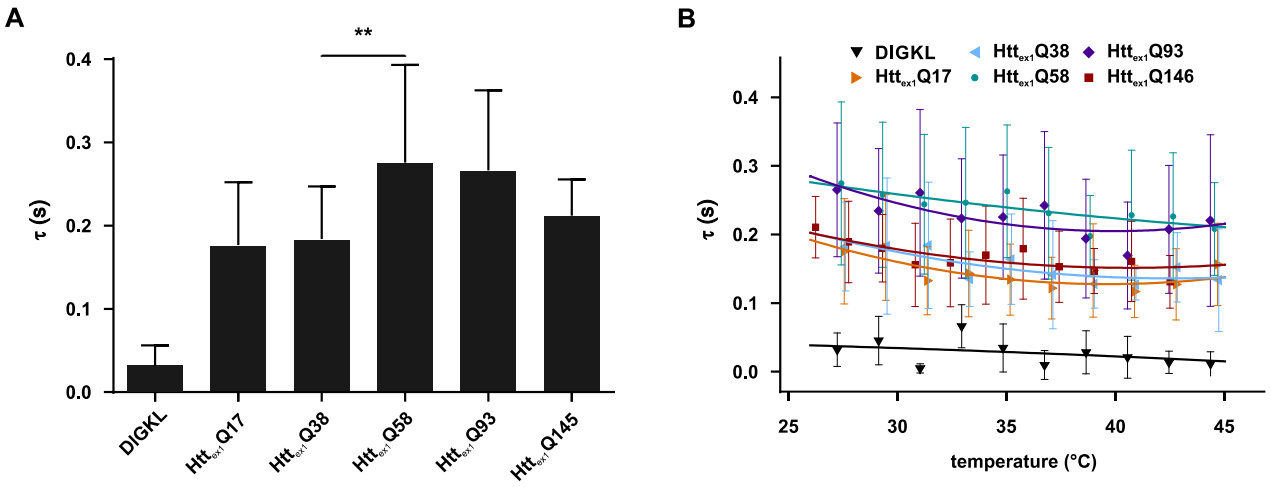

Relaxation kinetics of the Htt$_{ex1}$ collapse.

(*A*) Relaxation times of the collapse process upon a temperature jump from 25 °C to 27 °C for DIGKL (n = 6), Htt$_{ex1}$Q17 (n = 20), Htt$_{ex1}$Q38 (n = 26), Htt$_{ex1}$Q58 (n = 50), Htt$_{ex1}$Q93 (n = 38), and Htt$_{ex1}$Q146 (n = 20) in HeLa cells. Error bars depict the SD and the significance between different constructs were calculated by a one-way ANOVA with post-hoc Tukey test. ** $p < 0.01$ (*B*) Relaxation times of the collapse process for each 2 °C temperature jump during the temperature jump experiments. Error bars depict the SD. The dashed lines are meant as a guide to the eye.

Supplementary Figure S4

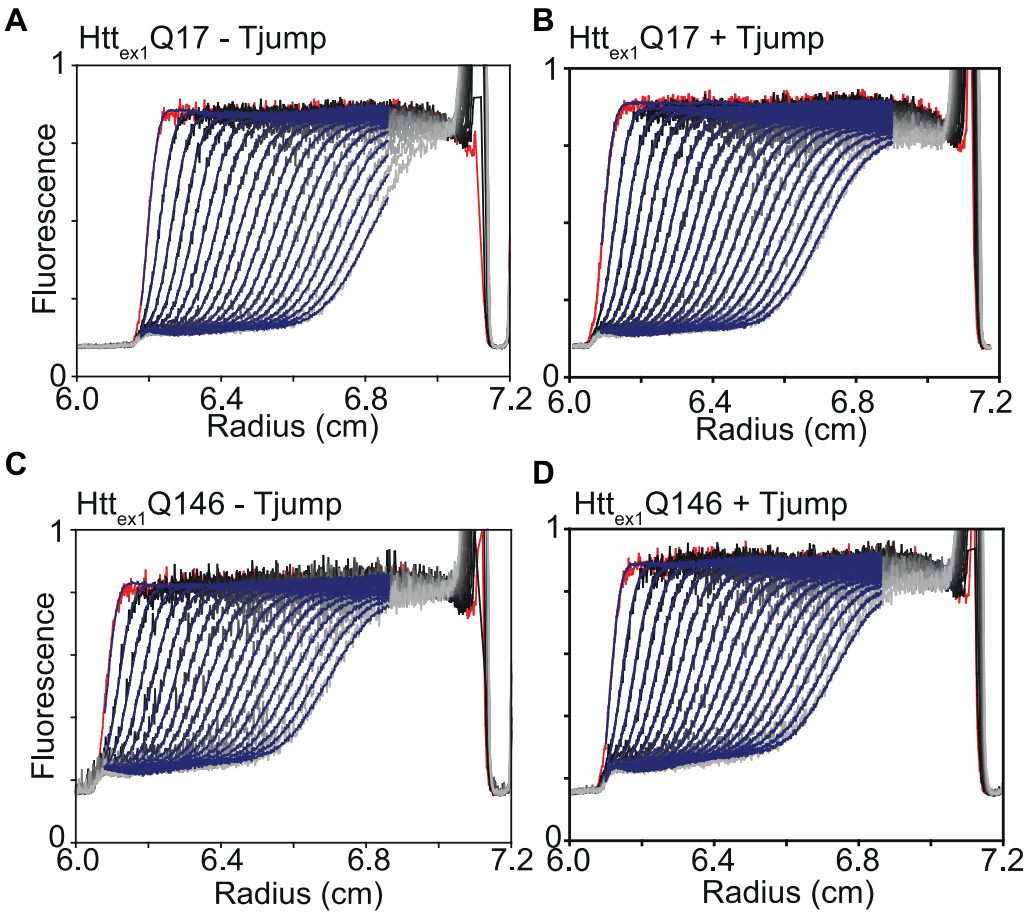

AUC fit analyses for Htt$_{ex1}$Q17 and Htt$_{ex1}$Q146 both with temperature jump (+ Tjump) and without (- Tjump).

Raw data of fluorescence scans are represented in grey with a red line indicating the first fluorescence scan. The fit analyses to the c(s) size distribution model are shown in blue. Representative data are shown for Htt$_{ex1}$Q17 (*A*), Htt$_{ex1}$Q17 + temperature jump (*B*), Htt$_{ex1}$Q146 (*C*) and Htt$_{ex1}$Q146 + temperature jump (*D*).

Supplementary Figure S5

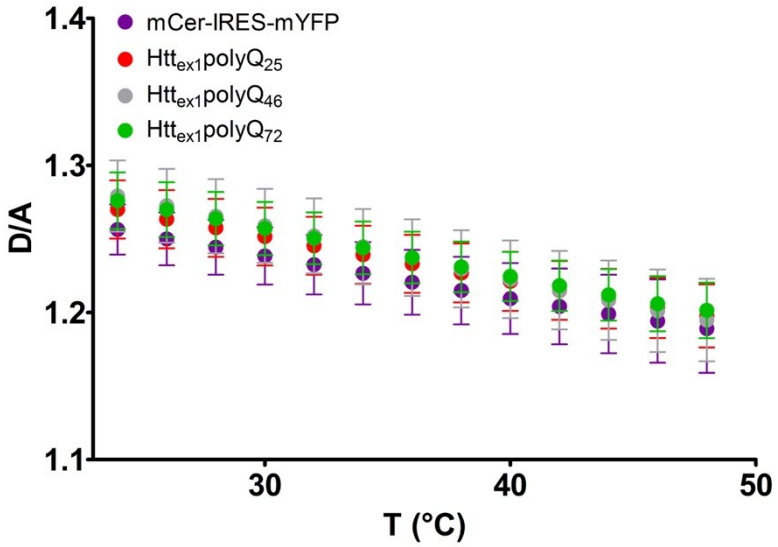

Tjump response of intermolecular FRET Htt$_{ex1}$ proteins.

Mean D/A ratios of mCer-Htt$_{ex1}$Q$_n$-mYFP and mCer-IRES-mYFP transfected cells in response to the Tjump assay. The data are shown as mean ± *s.d.*, $n = 20$.

Supplementary Table S1

Similarity based secondary structure prediction:

25°C		Helix (%)	Beta (%)	Irregular (%)	NRMSD
	AcGFP1-DIGKL-mCherry	6	49	46	0,21
	AcGFP1-Htt_{ex1}Q17-mCherry	9	48	43	0,26
	AcGFP1-Htt_{ex1}Q38-mCherry	14	39	47	0,16
	AcGFP1-Htt_{ex1}Q58-mCherry	14	39	47	0,22
37°C		Helix (%)	Beta (%)	Irregular (%)	NRMSD
	AcGFP1-DIGKL-mCherry	6	49	46	0,21
	AcGFP1-Htt_{ex1}Q17-mCherry	14	39	47	0,22
	AcGFP1-Htt_{ex1}Q38-mCherry	14	39	47	0,21
	AcGFP1-Htt_{ex1}Q58-mCherry	14	39	47	0,25
50°C		Helix (%)	Beta (%)	Irregular (%)	NRMSD
	AcGFP1-DIGKL-mCherry	6	49	46	0,19
	AcGFP1-Htt_{ex1}Q17-mCherry	14	39	47	0,28
	AcGFP1-Htt_{ex1}Q38-mCherry	9	41	50	0,28
	AcGFP1-Htt_{ex1}Q58-mCherry	9	41	50	0,37

Basis spectra derived secondary structure prediction:

25°C		Helix (%)	Beta (%)	Irregular (%)	Total (%)
	AcGFP1-DIGKL-mCherry	7	59	41	107
	AcGFP1-Htt_{ex1}Q17-mCherry	9	39	44	92
	AcGFP1-Htt_{ex1}Q38-mCherry	1	32	48	81
	AcGFP1-Htt_{ex1}Q58-mCherry	21	36	41	98
37°C		Helix (%)	Beta (%)	Irregular (%)	Total (%)
	AcGFP1-DIGKL-mCherry	8	58	42	108
	AcGFP1-Htt_{ex1}Q17-mCherry	6	37	41	84
	AcGFP1-Htt_{ex1}Q38-mCherry	7	34	44	85
	AcGFP1-Htt_{ex1}Q58-mCherry	15	38	48	101
50°C		Helix (%)	Beta (%)	Irregular (%)	Total (%)
	AcGFP1-DIGKL-mCherry	1	59	45	105
	AcGFP1-Htt_{ex1}Q17-mCherry	14	39	47	100
	AcGFP1-Htt_{ex1}Q38-mCherry	11	34	51	96
	AcGFP1-Htt_{ex1}Q58-mCherry	6	34	46	86

Secondary structure prediction for AcGFP1-DIGKL-mCherry and AcGFP1-$Htt_{ex1}Q_n$-mCherry proteins based on the CD spectra shown in Fig. 3.

Two secondary structure prediction results are shown: a basis spectra and a similarity based prediction method [2]. Predictions were performed using the CAPITO (http://capito.nmr.leibniz-fli.de/) software and reference data set [2].

SUPPLEMENTARY REFERENCES

1. K. Sathasivam, A. Neueder, T. A. Gipson, C. Landles, A. C. Benjamin, M. K. Bondulich, D. L. Smith, R. L. Faull, R. A. Roos, D. Howland, P. J. Detloff, D. E. Housman and G. P. Bates, *Proceedings of the National Academy of Sciences of the United States of America*, 2013, 110, 2366-2370.
2. C. Wiedemann, P. Bellstedt and M. Görlach, *Bioinformatics*, 2013, DOI: 10.1093/bioinformatics/btt278.